Southeastern Europe Tunnelling Conference (SETC-2025)
1-3 October 2025, Belgrade, Serbia

DOI: 10.5937/SETC25026M

Computer-aided ground modelling incorporating soil variability for geotechnical applications

Ksenija Micić[a,b], Hoang-Giang Bui[c] and Jelena Ninić[c]*

[a] University of Belgrade, Faculty of Mining and Geology, Department for Geotechnics, Belgrade, Serbia
[b] University of Belgrade, Faculty of Civil Engineering, Department of Geotechnical Engineering, Belgrade, Serbia; kmicic@grf.bg.ac.rs
[c] University of Birmingham, School of Engineering, Department of Civil Engineering, Birmingham, United Kingdom; b.hoanggiang@bham.ac.uk, j.ninic@bham.ac.uk

Abstract: This paper presents an end-to-end workflow for generating three-dimensional, voxel-based ground information model that seamlessly integrates geological complexity and soil-property variability into finite-element analyses. First, lithology is interpolated on a structured grid via Empirical Bayesian Kriging in ArcGIS Pro, producing a voxelized subsurface architecture. Next, spatial variability of key geotechnical parameters is characterized with conditional random fields using GSTools, utilizing borehole observations to ensure realistic site-specific conditions. All modelling components are stored and linked in NetCDF file, preserving dimensions and metadata, while allowing for the efficient data exchange. Finally, voxel-based ground information model is imported into a CutFEM solver for adaptive finite element simulations. We demonstrate the workflow on a synthetic excavation scenario, highlighting its computational efficiency and improved accuracy in predicting deformation compared to deterministic models. By automating the entire process and leveraging open data standards, this approach addresses interoperability challenges and enables engineers to incorporate uncertainty directly into numerical designs.

Keywords: GIM; soil variability; CutFEM; AMR

1. Introduction

In the past decades, as digital tools and technologies introduced an immersive need for digital transformation in engineering, the geotechnical community has witnessed a shift from traditional ways of ground modelling, such as 2D or block-based subsurface representations, toward 3D data-rich ground models that can capture geological and geotechnical complexity and directly be integrated with numerical solvers. Although many significant advancements have been made in this field (Erharter et al., 2023; Tian and Wang, 2024), there still appears to be a persistent gap between fully developed ground models and their practical application in geotechnical engineering, primarily due to poor interoperability among diverse data formats, software packages, and digital platforms.

While numerous high-quality research works on ground modelling (Erharter et al., 2023; Huang et al., 2022; Khan et al, 2023; Shi and Wang, 2022; Tian and Wang, 2023; Xie et al., 2023) mostly focus on just one aspect of the workflow (e.g. stratigraphy modelling, sparse data inference, BIM integration, FEM analysis), not many offer a simple, computationally efficient, and fully integrated 3D system that carries the ground model directly into FEM. Moreover, majority of the studies stop short of including the spatial variability of soil properties, which arises from complex geological processes (Phoon and Kulhawy, 1999a) and represents an inevitable part of ground characterization. It can effectively be assessed employing the Random Field Theory (Chen et al., 2024; He et al., 2022; Huang et al., 2020; Pan and Dias, 2017; Vanmarcke, 1977). To fully pair all the unknowns with the 'known' ground information, it is of great importance to constrain the stochastic predictions with the actual field

*Corresponding author: kmicic@grf.bg.ac.rs (K. Micić).

observation data, which is achievable by conditioning the random simulations for the known values at specific locations (Gong et al., 2018; Huang et al., 2020; Hu et al., 2025; Wang et al., 2024; Xie et al., 2023; Zhao et al., 2023).

Numerical analysis plays an important role in initial assessment of settlement-induced construction process. For tunnelling application, CutFEM is a method of choice for design of tunnel track (Bui et al., 2023). This approach allows for independent modelling of analysis components. In particular, the ground can be modelled using regular geometry without initial generation of boundary fitted excavation domain. This fits naturally with ground data defined on a structured grid and enables seamless integration of ground information model (GIM) during the simulation.

In this work we present an end-to-end workflow that: (1) uses borehole data to produce a 3D lithology model in ArcGIS using Empirical Bayesian Kriging, (2) enriches the lithology voxel model with conditional random fields of key soil properties to reach a holistic voxel-based GIM, and (3) seamlessly incorporates GIM into Kratos-based CutFEM solver. The main objective of the study is to establish a reproducible, interoperable and automated pipeline for adaptive FEM analysis using 3D spatially variable ground models.

2. Voxel-based ground model

2.1. Field investigation data

Geotechnical datasets from individual projects are typically limited in size and often irregularly distributed, due to constraints of budget, schedule, or access (Phoon et al. 2023, Wang and Tian, 2023). Even though geotechnical standards prescribe a wide range of investigation methods, each offering its own benefits for characterizing ground conditions, the borehole drilling remains the cornerstone technique. It provides multiple streams of information directly from subsurface materials, including lithology, groundwater conditions, and sampling for laboratory testing.

In this study, boreholes form the foundational data layer from which all the other ground modelling components are derived. Whilst the entire framework is built on synthetic data, great attention has been put into configuring the inputs as realistically as possible, ensuring that every subsequent analysis and simulation retains physical and geotechnical validity.

To that end, Fig. 1 shows 50 random synthetic boreholes distributed over the domain of interest measuring 400 × 300 × 60 m in X, Y and Z, respectively. Each digital borehole is organized into distinct elements, with each element carrying its own characteristic set of data (Fig. 1). To be able to achieve full connectivity between the distinct elements, parent-child mappers are established.

2.2. Lithology modelling in GIS

2.2.1. Empirical Bayesian Kriging

Lithology modelling is conducted using the ArcGIS Pro's Geostatistical Analyst toolbox that contains a suite of tools for data analysis, interpolation and validation, among which Empirical Bayesian Kriging (EBK) stands out as an advanced and well-equipped algorithm for lithology spatial delineation (Esri, 2025).

Empirical Bayesian Kriging (EBK) is a geostatistical interpolation approach that embeds the iterative semivariogram fitting within a Bayesian framework and combines two underlying models within a unified computational procedure - an intrinsic random function kriging (IRFK) component and a linear mixed model (LMM) component. In the computational model, observations z_i at locations s_i are expressed as:

$$z_i = y(s_i) + \varepsilon_i, \qquad i = 1, \dots, K \tag{1}$$

where $y(S)$ is the underlying Gaussian spatial process, ε_i denotes measurement error and K is the number of observations (Gribov and Krivoruchko, 2020; Krivoruchko and Gribov, 2019).

The core EBK workflow first estimates semivariogram parameters using the restricted maximum likelihood method (REML), then produces multiple unconditional simulations to build an empirical prior of parameter sets. Each set is weighted by its likelihood of producing the observed data, and final predictions at unsampled locations are obtained by averaging the individual predictions generated by each parameter set, using the weights. For large datasets, the input is divided into overlapping subsets, each processed independently. In full 3D mode in ArcGIS Pro, the EBK logic is preserved while adapting distance metrics and search neighbourhood definitions to three dimensions (Esri, 2025).

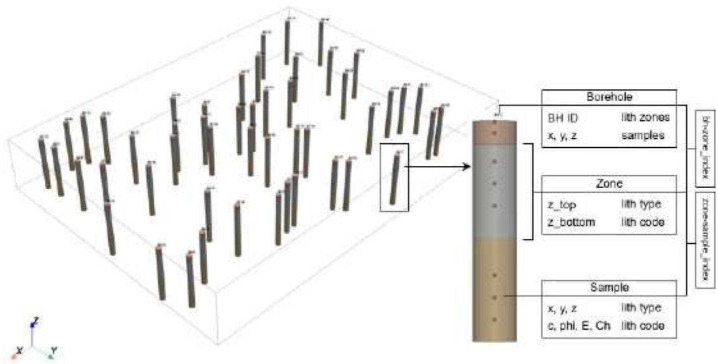

Fig. 1. Borehole distribution in 3D domain of interest. Digital borehole contents presented on the right.

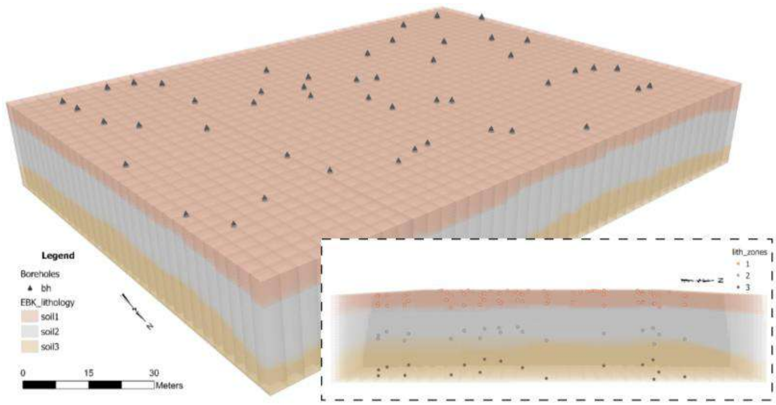

Fig. 2. 3D lithology model generated using ArcGIS Pro's EBK, with an excerpt of a vertical view showing the zone points used for modelling.

2.2.2. Voxel-based lithology model

We produce the 3D lithology model using the ArcGIS Pro's EBK tool in several steps. First, we prepare the input lithology data as point feature layer containing 3D spatial coordinates, as well as lithology index (Fig. 2). Then, we configure the EBK model: semivariogram type, subset size, number of simulations. This part also allows for data transformation, if needed. After defining the vertical anisotropy with trend removal and elevation inflation factor, we set the search neighbourhood parameters: radius, sectorization scheme and number of neighbours. Next, the tool is being run and the performance is evaluated through error diagnostics. Final step includes reclassifying EBK continuous prediction into discrete lithology units.

Upon execution, the output is stored as a geostatistical layer that shows a horizontal transect at a given location. It encapsulates the source dataset path, all EBK parameters used for the interpolation, and metadata for subsequent mapping or re-evaluation. Geostatistical layer is further used to generate a multidimensional voxel-based raster that stores volumetric data in NetCDF format (see Section 2.4.). In this study, we employ voxels for building and representing the digital ground model, which seamlessly integrate with subsequent modelling components. The entire workflow is fully automated with ArcPy, Esri's comprehensive Python library for spatial analysis, data management, and conversion (Esri, 2025). The lithology model derived from synthetic digital borehole data (Section 2.1.) is presented in Fig. 2.

2.3. Soil spatial variability

2.3.1. Conditional random field (CRF) generation in GSTools

The conditional simulation process can reliably be executed in GSTools (Müller et al., 2022), which is an open-source Python library designed for efficient geostatistical modelling and spatial random field simulation. A CRF is generated following a three-step procedure that includes: 1) computing kriging weights and generating a kriged field, 2) generating an unconditional realization of a random field, and 3) conditioning the unconditional random field with the kriging correction for the observed measurements, as detailed below.

Regardless of the generation technique, an unconditional simulation greatly depends on a covariance model whose definition typically involves specifying variance (σ^2), nugget (n), correlation length (ℓ), and a chosen form of correlation function $cor(h)$. Once a variogram model is in place, a common way to simulate a Gaussian random field is by utilizing the Randomization method (Heße et al., 2014; Kraichnan, 1970) that employs the variogram model's spectral density to simulate a Wiener process in the Fourier domain. In this approach, the field $U_u(x)$ is estimated with:

$$U_u(x) = \sqrt{\frac{\sigma^2}{N}} \sum_{i=1}^{N} \left(a_i cos(k_i \cdot x) + b_i sin(k_i \cdot x) \right) \tag{2}$$

where N is the number of Fourier modes used in the simulation, a_i and b_i are independent standard normal random variables ($\mathcal{N}(0,1)$), and k_i represent independent random wave vectors sampled from the spectral density corresponding to the variogram model.

Then, with kriging, the unknown values of a field U_k at a spatial point x_0 are estimated by applying the weighting factor λ_i to the observed values Z_1, Z_2, ..., Z_n at spatial points x_1, x_2, ..., x_n:

$$U_k(x_0) = \sum_{i=1}^{N} \lambda_i Z_i = \sum_{i=1}^{N} \lambda_i(x_0) Z(x_i) \tag{3}$$

for which N is the number of observations, and the weights are determined by minimizing the kriging error variance σ_e^2.

Thus, a conditional random field can generally be observed as a set of three components, which make up the CRF generation process:

$$U_c(x) = U_u(x) + \left(U_k(x) - U_{ks}(x) \right) \tag{4}$$

where x represents a spatial location, $U_u(x)$ refers to the unconditional random field, $U_k(x)$ denotes the kriging estimate based on measured data at their locations x_i for $i = 1, 2, ..., N$, and $U_{ks}(x)$ is the kriging estimate based on the simulated values from the unconditional field at the same locations.

2.3.2. Conditional realizations of soil properties

Here, we generate conditional realizations of four soil properties considered most relevant for conducting numerical analysis – cohesion, internal friction angle, Young's modulus and plastic hardening modulus, for each soil type. For assessing the domain of interest's spatial variability, we fully utilize the previously presented workflow by conditioning the stochastic simulation for the measurement data obtained from soil samples. Table 1 shows a set of statistical parameters used for CRF simulation in soil 1, 2 and 3, which are adopted based on author's previous work (Bui and Meschke, 2020).

Table 1. Set of adopted soil properties from soil samples

	Soil 1			Soil 2			Soil 3		
	min	max	μ	min	max	μ	min	max	μ
c (kPa)	24.09	32.88	28.42	26.00	34.93	30.48	82.23	91.76	86.81
φ (º)	26.05	30.95	28.29	28.02	32.95	30.59	30.01	34.99	32.82
E (MPa)	25.03	31.98	28.17	42.09	49.95	45.99	60.07	69.96	65.38
Ch (kPa)	27.05	32.98	30.14	40.00	47.97	44.13	57.06	64.95	61.02

Soil properties' distribution is modelled using the exponential covariance model paired with ordinary kriging routine, conditioning the simulation at 400 measurement points in total. The simulation is performed on a structured voxel grid inherited from the lithology model. Generated CRFs of soil properties preserve the domain's original spatial structure, realistically evaluating their variability, as shown in Fig. 3. Generally, soil properties' values perform greater variability in horizontal, than in vertical direction, clustering over the lengths defined by the correlation structure, while simultaneously respecting the known values from the borehole samples. Higher fluctuations and sharper transitions in cohesion and Young's modulus values at the interface of soil 2 and soil 3 are expected to form stress concentration zones along the contact.

2.4. Ground Information Model

2.4.1. Voxelization and Network Common Data Format

Voxel-based ground models greatly benefit the ground modelling procedure with their ability to refine the resolution at multiple scales, represent heterogeneous geological information across the domain and incorporate semantic data (Khan et al., 2023). Voxel represents a 3D cell or a cube that can carry volumetric and semantic information. Depending on the model complexity and further integration schemes, voxels can either be of uniform or differing size in three dimensions. Usually, a set of information that a voxel carries is assigned to its centre point, offering simplicity in voxel grid and data reconstruction across different modelling tools and software.

Since ArcGIS Pro produces voxel-based EBK models in NetCDF format (see section 2.2.), it is recognized as convenient, efficient and promising way of constructing GIM. NetCDF (Network Common Data Form) is a standardized, array-oriented file format designed for storing and exchanging diverse scientific datasets (NSF Unidata, 2025; Rew and Davis, 1990). It is self-describing, portable across platforms, and scalable, enabling efficient access to subsets of large datasets without requiring the entire file loading.

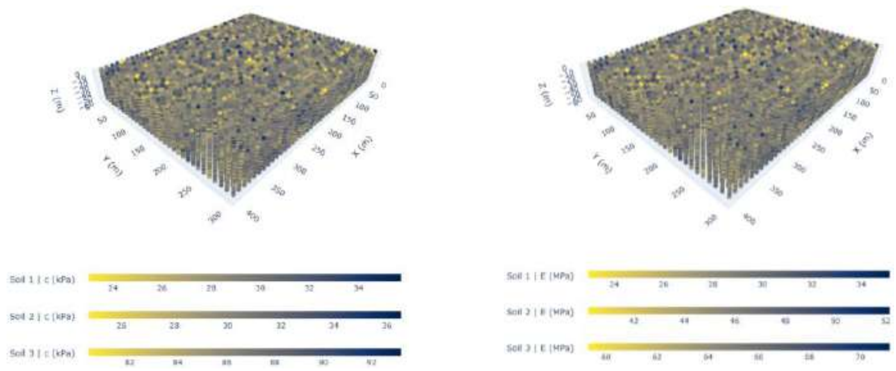

Fig. 3. 3D conditional realization of cohesion on the left and Young's modulus on the right (the other two CRFs are left out from visualization for the space sake).

2.4.2. GIM structure

GIM is structurally and hierarchically derived using the bottom-up approach (Fig. 4), such that each modelling component (group, subgroup) is generated in a staged workflow by consuming the data output of the previous stage, before writing its own results back into NetCDF. The starting layer is represented by the field observation data and its correlated metadata, stored as a root group. This non-gridded dataset is organized within three primary dimensions each corresponding to the borehole investigation elements and storing their specific variables (Fig. 1). Next, the GIS lithology voxel model is created loading the root-level variables (borehole coordinates, zone elevations, lithology types) and following the procedure described in Section 2.2. Besides the GIS projection data, this gridded model stores a number of voxels used for its construction, represented by the length of each dimension (based on voxel size), voxel centre coordinate arrays and the domain of interest bounding box. Within this group, the primary variable is a three-dimensional integer array *lithology[z,y,x]*, consisting of the interpolated lithology codes at each voxel centre. Built on top of the GIS voxel model, the CRF subgroup represents spatially varying soil parameters and their gradients, essentially using sample data for simulating the parameters on the voxel grid inherited from the lithology model. Soil parameter CRFs are generated as described in Section 2.3., resulting in a suite of 3D float arrays, each augmented with its own metadata (such as units and descriptions).

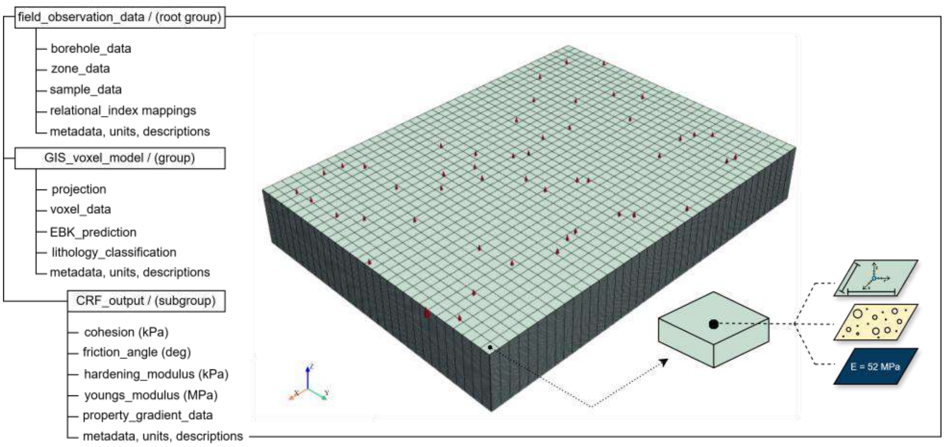

Fig. 4. GIM structure and voxel contents.

GIM constructed in this manner offers: a) full traceability – starting from the investigation data, and deriving multiple models in stages, b) modularity – modelling components are organized into groups of different characteristics, and c) reusability – groups can be accessed and used separately. Owing to its geometrical and structural features, voxel-based GIM provides all the necessary input for numerical modelling, allowing for seamless interoperability with FEM solvers, as presented in the following sections.

3. Finite element modelling with ground model input

3.1. Computational model for soils

Soil is a typical porous media, characterized by the void ratio between the solid skeleton and the matrix water. This ratio is often denoted as porosity. Depending on the working condition, soil can include air, especially when compressed air is flushed into the tunnel chamber during maintenance. Nevertheless, in the normal condition, soil below the groundwater table is considered to be fully saturated and fully dried above the groundwater level, i.e., drain condition. In terms of energy, the equilibrium state of the soil mixture is characterized by the balance of momentum and the mass balance equation. The whole set of equation is time dependent, and the discretised weak form can be integrated in time using Generalized Newmark-α method (Chung and Hulbert, 1993). For the details of the saturated soils formulation, the reader is referred to Nagel and Meschke (2010) and Bui et al. (2022).

3.2. CutFEM for excavation analysis

Robust treatment of material removal procedure is crucial for the success of excavation analysis. In the traditional FEM analysis, material removal is characterised by element deactivation. Although simple, this approach does not allow to fine grain control the removal domain, which is governed by the element size. To do that, one must either refine the mesh or using a load reduction technique, e.g., CCM (Pham et al., 2025). In contrast, CutFEM treats the material removal at the integration point by applying suitable penalisation factor. By using adaptive quadrature, the material point can be penalised as prescribed by the cut boundary. An exemplary demonstration of this concept is illustrated in Fig. 5 (Left) for material point penalisation and in Fig. 5 (Right) for adaptive quadrature.

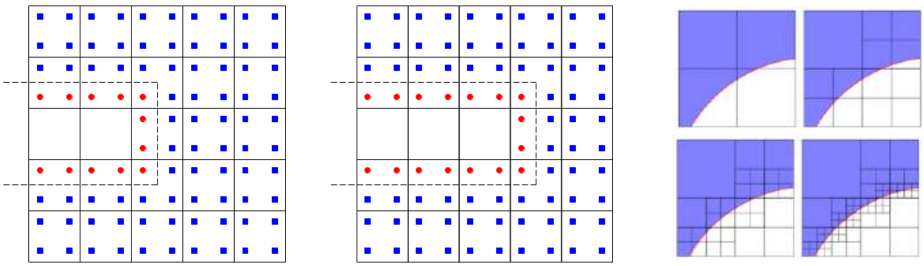

Fig. 5. (Left) Illustration of material point penalisation in excavation analysis with CutFEM. Red (•) dots are the inactive points and blue (■) dots are the active points; (Right) Illustration of CutFEM adaptive quadrature.

3.3. Adaptive mesh refinement

The stark change in the gradient of the stress field typically signifies a reduction of local accuracy (Szabó and Babuška, 2011), hence it is necessary to refine the mesh locally in this area. The spatially variable ground model often contains abrupted changes in the material properties, as presented in

Section 2.3. In this work, the Young's modulus E is selected to drive the mesh refinement due to its direct influence on the stress level. Following that, the gradient of E is used to decide if a refinement is needed for an element if $\|grad\ E\| > \epsilon_E$.

The mesh refinement procedure based on subdivision approach (Burstedde et al., 2011) is used due to its simplicity and readily available of high-performance package, i.e., p4est. This technique is based on binary subdivision in space. For 3D problem, a number of eight sub-cells will be created for a box grid cell of the structured grid. This division introduces hanging nodes. The displacement at the hanging nodes must be constrained to maintain the continuity of the displacement field (Bui et al., 2022).

The refinement criterion requires the calculation of grad E by the ground information model. In case it is not available, grad E can be approximated as

$(grad\ E)_{i,j,k} = \frac{1}{2}\left[\frac{E_{i+1,j,k} - E_{i-1,j,k}}{dx}, \frac{E_{i,j+1,k} - E_{i,j-1,k}}{dy}, \frac{E_{i,j,k+1} - E_{i,j,k-1}}{dz}\right]$, in which i, j, k is the index of the grid cell and dx, dy, dz are the size of a cell in the Cartesian directions respectively. It is noted that this scheme possesses second-order accuracy.

3.4. GIM integration

Integration of the GIM into geotechnical analysis is straightforward, providing that it can provide the parameter evaluation spatially. Having said that, a material parameter χ can be considered as mapping χ: R3 → R. In the voxel-based GIM described in Section 2.4.3., the material field value is stored in the discrete form at the grid vertices. Hence, the level set approach, i.e., using finite element shape function, can be employed to interpolate the value in space. The parameter setting problem reduces to global search of a grid cell which contains the spatial point, then determining its local coordinates. The final step is to interpolate the grid value based on shape functions evaluated at the local point.

4. Numerical example

To demonstrate the computational approach in this work, we set up a tunnel analysis with the background mesh of size 400 × 300 m. As for the ground model, it is constructed in full accordance with the procedure presented earlier (see Section 2.), such that it covers the domain of interest shown in Section 2.1. It consists of 39 401 voxels total, all equally dimensioned in x, y and z with 10, 10, 2 m, respectively. Each voxel stores the specific geological-geotechnical dataset assigned to its centre point, making the data exchange simple and straightforward. There are three different soil types delineated within the ground model (soil1, soil2 and soil3, see Fig. 2), and each one of them is characterized with spatially variable soil properties derived using conditional realizations of random field (Section 2.3).

For simplicity, only drained analysis is performed, and simple deactivation of the tunnel is used to simulate the excavation sequence. In this approach, the soil is deactivated along the tunnel track by setting the quadrature weight of the integration point within the excavation region to 10^{-12}. Subsequently, the tunnel lining is activated and tied with the background mesh. The analysis step is done by letting the soil consolidates freely. The constitutive law is selected as linear elastic for both the lining segment and the soil, in which the modulus of the lining is 3×10^{10}. As a result, the analysis will converge in at most one iteration.

It is well known in literature that Young's modulus (E) is one of the most sensitive parameters in predicting settlement in the tunnel analysis problem, e.g., (Nguyen et al., 2024; Ninić et al., 2015). In Ninić et al. (2015), the global sensitivity analysis employing FEM is analysed for E in each soil layer. In Nguyen et al. (2024), the feature importance analysis is performed on the lining-soil interaction model. The results show that E is the most important feature to affect the lining displacement. Hence, we select E as the primary parameter to study the effect of soil variability in numerical analysis.

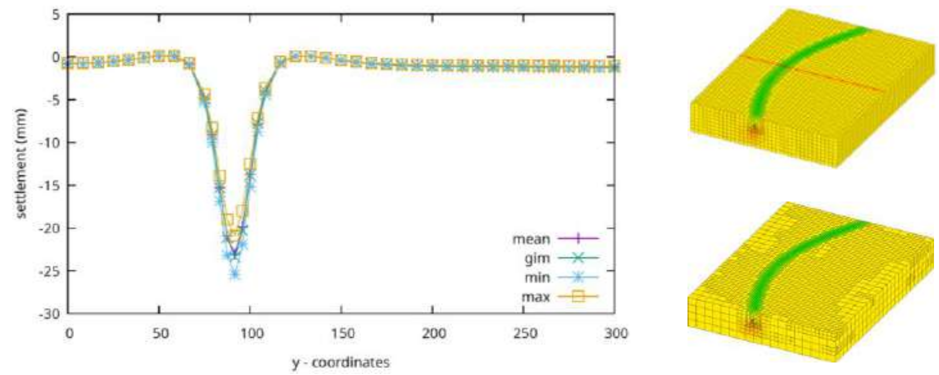

Fig. 6. (Left) Obtained settlements for deterministic and GIM analyses and (Right) Settlement field of the analysis with mean E in each soil layer (Top left) and with soil variability (Bottom left).

Fig. 6 (Right) presents the settlement field of both analyses using mean values and with soil variability respectively. It also shows the meshes used for the analysis with deterministic soil parameters and with soil variability. Due to the change in Young's modulus fields, the mesh is refined for the analysis with GIM. In Fig. 6 (Left), the settlement is sampled in the middle section (red line) and compared with the deterministic analyses using the minimum and maximum values of the Young's modulus field. As expected, the results using mean values and GIM are bounded by the curves with minimum and maximum values. The difference in the largest settlement of "mean" and "GIM" results is ~ 1.3%. We anticipate that the fluctuation in the variability model compensates each other, thus giving very closed results to the "mean" analysis. Nevertheless, the "GIM" analysis is able to capture local changes in the stress field, as visualised in Fig. 7 for σ_{zz} and Fig. 10 for vertical stress sampling at points along the tunnel. This observation verifies an important theoretical aspect, that the displacement field is the integral of the strain and is generally smoother than the stress field, see Fig. 6 (Right).

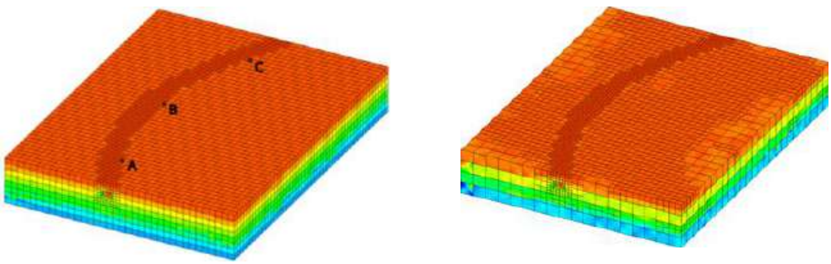

Fig. 7. σ_{zz} field of the analysis with mean E in each soil layer (left) and with soil variability (right)

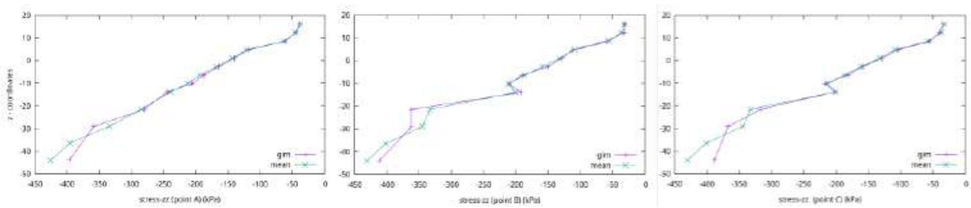

Fig. 8. Vertical stress field sampling at point A, B and C, see Fig. 7.

5. Conclusions

This study presents the incorporation of soil variability into geotechnical analysis via ground information model. It underpins the effort to account for uncertainty in geotechnical design, opening a new paradigm for expanding the applicability and improving the reliability of numerical analysis in engineering. The proposed approach is conducted by establishing an efficient data exchange interface between voxel-based ground model and finite element analysis. By providing the procedure to import spatial data from NetCDF of GIM and approximate the field gradient, the method enables mesh refinement technique that enhances the computational accuracy.

To demonstrate the methodology, the tunnel excavation analysis is carried out employing the CutFEM concept for material removal. This approach is shown to be effective, since structured grid is used consistently for both data representation and simulation mesh. The results reveal that the GIM analysis can capture localised changes in the stress field, offering more detailed look into soil-structure interaction. Future work includes studying the effect of soil parameters in nonlinear analyses, incorporating realistic constitutive models for soil behaviour, as well as enriching and updating GIM with a bigger scope of relevant geological and geotechnical data. In terms of applicability, the computational approach can then be relevant for other types of analysis, such as foundation excavation and incorporation of buildings and structures.

Acknowledgements

The first author acknowledges the support of the Science Fund of the Republic of Serbia through project #345 - Digital and Numerical Model Integration for Optimization in Geotechnics – DiNum-GEO. The second author is supported by Marie Sklodowska-Curie project TwinSSI (UKRI – EP/Z001072/1).

References

Bui, H-G. and Meschke, G. 2020. A parallelization strategy for hydro-mechanically coupled mechanized tunneling simulations. *Computer and Geotechnics*, 120, 103378. https://doi.org/10.1016/j.compgeo.2019.103378

Bui, H.-G., Schillinger, D., Zendaki, Y., Meschke, G., 2022. A CutFEM based framework for numerical simulations of machine driven tunnels with arbitrary alignments. *Computers and Geotechnics*, 144, 104637. https://doi.org/10.1016/j.compgeo.2022.104637

Bui, H.-G., Cao, B.-T., Freitag, S., Hackl, K., Meschke, G., 2023. Surrogate modeling for interactive tunnel track design using the cut finite element method. *Engineering with Computers*, 39, 4025–4043. https://doi.org/10.1007/s00366-023-01867-y

Burstedde, C., Wilcox, L., and Ghattas, O., 2011. P4est: Scalable algorithms for parallel adaptive mesh refinement on forests of octrees. *SIAM Journal on Scientific Computing*, 33(3), 1103–1133. https://doi.org/10.1137/100791634

Chen, X. J., Fang, P. P., Chen, Q. N., Hu, J., Yao, K., Liu, Y. 2024. Influence of cutterhead opening ratio on soil arching effect and face stability during tunnelling through non-uniform soils. *Underground Space*, 17, 45–59. https://doi.org/10.1016/j.undsp.2023.11.003

Chung, J., Hulbert, G. M., 1993. A time integration algorithm for structural dynamics with improved numerical dissipation: The generalized-α method. *Journal of Applied Mechanics*, 60(2), 371–375. https://doi.org/10.1115/1.2900803

Esri. What is empirical Bayesian kriging? ArcGIS Pro documentation. Available online: https://pro.arcgis.com/en/pro-app/latest/help/analysis/geostatistical-analyst/what-is-empirical-bayesian-kriging-.htm (accessed on 1 June 2025)

Esri. What is ArcPy? ArcGIS Pro documentation. Available online: https://pro.arcgis.com/en/pro-app/3.4/arcpy/get-started/what-is-arcpy-.htm (accessed on 1 June 2025)

Gong, W., Juang, C.H., Martin, J. R., Tang, H., Wang, Q., Huang, H. 2018. Probabilistic analysis of tunnel longitudinal performance based upon conditional random field simulation of soil properties. *Tunnelling and Underground Space Technology*, 73, 1–14. https://doi.org/10.1016/j.tust.2017.11.026

Gribov, A., and Krivoruchko, K. 2020. Empirical Bayesian kriging implementation and usage. *Science of the Total Environment*, 722, 137290. https://doi.org/10.1016/j.scitotenv.2020.137290

Heße, F., Prykhodko, V., Schlüter, S., Attinger, S. 2014. Generating random fields with a truncated power-law variogram: A comparison of several numerical methods. *Environmental Modelling & Software*, 55, 32–48. https://doi.org/10.1016/j.envsoft.2014.01.013

He, Z., Xu, H., Gardoni, P., Zhou, Y., Wang, Y., Zhao, Z. 2022. Seismic demand and capacity models and fragility estimates for underground structures considering spatially varying soil properties. *Tunnelling and Underground Space Technology*, 119, 104231. https://doi.org/10.1016/j.tust.2021.104231

Huang, L., Zhang, Y., Lo, M., Cheng, Y. 2020. Comparative study of conditional methods in slope reliability evaluation. *Computers and Geotechnics*, 127, 103762. https://doi.org/10.1016/j.compgeo.2020.103762

Hu, L., Kasama, K., Wang, G., Takahashi, A. 2025. Assessing the influence of geotechnical uncertainty on existing tunnel settlement caused by new tunnelling underneath. *Tunnelling and Underground Space Technology*, 155(Pt 1), 106189. https://doi.org/10.1016/j.tust.2024.106189

Khan, M. S., Kim, I. S., Seo, J. W. 2023. A boundary and voxel-based 3D geological data management system leveraging BIM and GIS. *International Journal of Applied Earth Observation and Geoinformation*, 118, 103277. https://doi.org/10.1016/j.jag.2023.103277

Kraichnan, R. 1970. Diffusion by a random velocity field. *Physics of Fluids*, 13, 22–31. https://doi.org/10.1063/1.1692799

Krivoruchko, K., Gribov, A. 2019. Evaluation of empirical Bayesian kriging. *Spatial Statistics*, 32, 100368. https://doi.org/10.1016/j.spasta.2019.100368

Müller, S., Schüler, L., Zech, A., Heße, F. 2022. GSTools v1.3: A toolbox for geostatistical modelling in Python. *Geoscientific Model Development, 15*, 3161–3182. https://doi.org/10.5194/gmd-15-3161-2022

Nagel, F., Meschke, G., 2010. An elasto-plastic three phase model for partially saturated soil for the finite element simulation of compressed air support in tunnelling. *International Journal for Numerical and Analytical Methods in Geomechanics*, 34(6), 605–625. https://doi.org/10.1002/nag.828

Nguyen, T.T, Cao, B.T, Pham, V.V, Bui, H.G., Do, N.A, 2024, Design optimization of quasi-rectangular tunnels based on hyperstatic reaction method and ensemble learning. *Journal of Rock Mechanics and Geotechnical Engineering*. https://doi.org/10.1016/j.jrmge.2024.10.020

Ninić, J., Meschke G. 2015. Model update and real-time steering of tunnel boring machines using simulation-based meta models. *Tunnelling and Underground Space Technology*, 45, 138–152. https://doi.org/10.1016/j.tust.2014.09.013

NSF Unidata. Network Common Data Form (NetCDF). Available online: https://www.unidata.ucar.edu/software/netcdf/ (accessed on 1 June 2025)

Pan, Q. J., Dias, D. 2017. Probabilistic evaluation of tunnel face stability in spatially random soils using sparse polynomial chaos expansion with global sensitivity analysis. *Acta Geotechnica*, 12, 1415–1429. https://doi.org/10.1007/s11440-017-0560-9

Pham, V.-V., Do, N.-A., Osinski, P., Do, N.-T., Bui, H.-G., Cao, B.-T., Nguyen, T.-T., Dias, D., 2025. Effect of the pile foundation and soil constitutive models on the behavior of twin circular tunnels considering the deconfinement process. *Environmental Earth Sciences*. https://doi.org/10.1007/s12665-025-12365-3

Rew, R. K., Davis, G. P. 1990. NetCDF: An interface for scientific data access. *IEEE Computer Graphics and Applications*, 10(4), 76–82. https://doi.org/10.1109/38.56302

Shooib Khan, M., Kim, I. S., Seo, J. W. 2023. A boundary and voxel-based 3D geological data management system leveraging BIM and GIS. *International Journal of Applied Earth Observation and Geoinformation*, 118, 103277. https://doi.org/10.1016/j.jag.2023.103277

Shi, C., Wang, Y. 2022. Data-driven construction of three-dimensional subsurface geological models from limited site-specific boreholes and prior geological knowledge for underground digital twin. *Tunnelling and Underground Space Technology*, 126, 104493. https://doi.org/10.1016/j.tust.2022.104493

Szabó, B., Babuška, I., 2011. Introduction to finite element analysis: Formulation, verification and validation. *Wiley*.

Tian, H., Wang, Y. 2023. Data-driven and physics-informed Bayesian learning of spatiotemporally varying consolidation settlement from sparse site investigation and settlement monitoring data. *Computers and Geotechnics*, 157, 105328. https://doi.org/10.1016/j.compgeo.2023.105328

Vanmarcke, E. H. 1977. Probabilistic modeling of soil profiles. *Journal of the Geotechnical Engineering Division, ASCE*, 103(11), 1227–1246. https://doi.org/10.1061/AJGEB6.0000517

Wang, L., Pan, Q., Wang, S. 2024. Data-driven predictions of shield attitudes using Bayesian machine learning. *Computers and Geotechnics*, 166, 106002. https://doi.org/10.1016/j.compgeo.2023.106002

Wang, Y., Tian, H.-M. 2024. Digital geotechnics: From data-driven site characterisation towards digital transformation and intelligence in geotechnical engineering. *Georisk: Assessment and Management of Risk for Engineered Systems and Geohazards*, 18(1), 8–32. https://doi.org/10.1080/17499518.2023.2278136

Xie, P., Chen, K., Skibniewski, M., Wang, J., Luo, H. 2023. Parametric geological model update and probabilistic analysis of shield tunnel excavation: A borehole-based conditional random fields approach. *Computers and Geotechnics*, 157, 105349. https://doi.org/10.1016/j.compgeo.2023.105349

Zhao, C., Gong, W., Juang, C.-H., Tang, H., Hu, X., Wang, L. 2023. Optimization of site exploration program based on coupled characterization of stratigraphic and geo-properties uncertainties. *Engineering Geology*, 317, 107081. https://doi.org/10.1016/j.enggeo.2023.107081